# A Subfamily of Bacterial Ribokinases Utilizes a Hemithioacetal for Pyridoxal Phosphate Salvage

Matthew B. Nodwell,[†] Maximilian F. Koch,[†] Ferdinand Alte,[†] Sabine Schneider,*[‡]
and Stephan A. Sieber*[†]

[†]Organic Chemistry II, Centre for Integrated Protein Science CIPSM, Institute of Advanced Studies, and [‡]Biochemistry, Department of Chemistry, Technische Universität München, Lichtenbergstrasse 4, 85747 Garching, Germany

S *Supporting Information*
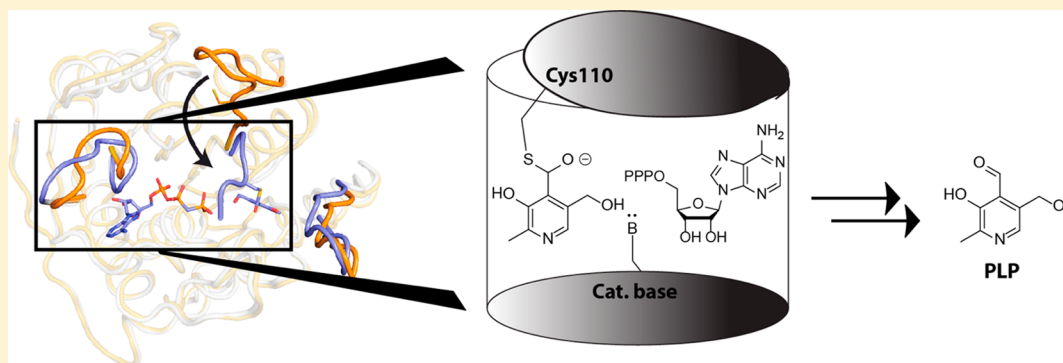
ABSTRACT: Pyridoxal 5′-phosphate (PLP) is the active vitamer of vitamin B$_6$ and acts as an essential cofactor in many aspects of amino acid and sugar metabolism. The virulence and survival of pathogenic bacteria such as *Mycobacterium tuberculosis* depend on PLP, and deficiencies in humans have also been associated with neurological disorders and inflammation. While PLP can be synthesized by a de novo pathway in bacteria and plants, most higher organisms rely on a salvage pathway that phosphorylates either pyridoxal (PL) or its related vitamers, pyridoxine (PN) and pyridoxamine (PM). PL kinases (PLKs) are essential for this phosphorylation step and are thus of major importance for cellular viability. We recently identified a pyridoxal kinase (SaPLK) as a target of the natural product antibiotic rugulactone (Ru) in *Staphylococcus aureus*. Surprisingly, Ru selectively modified SaPLK not at the active site cysteine, but on a remote cysteine residue. Based on structural and biochemical studies, we now provide insight into an unprecedented dual Cys charge relay network that is mandatory for PL phosphorylation. The key component is the reactive Cys 110 residue in the lid region that forms a hemithioacetal intermediate with the 4′-aldehyde of PL. This hemithioacetal, in concert with the catalytic Cys 214, increases the nucleophilicity of the PL 5′-OH group for the inline displacement reaction with the γ-phosphate of ATP. A closer inspection of related enzymes reveals that Cys 110 is conserved and thus serves as a characteristic mechanistic feature for a dual-function ribokinase subfamily herein termed CC-PLKs.

■ INTRODUCTION

Vitamin B$_6$ is a collective term for three pyridine analogues called pyridoxal (PL), pyridoxine (PN), and pyridoxamine (PM) (Figure 1).

These vitamers are precursors to pyridoxal-5′-phosphate (PLP), which is an essential cofactor involved in more than 140 enzymatic reactions, or approximately 4% of all classified activities.[1,2] It has been shown that PLP is crucial for virulence and survival of pathogenic bacteria like *Streptococcus pneumoniae*,[3] *Helicobacter pylori*,[4] *Mycobacterium tuberculosis*,[5] and *Vibrio cholerae*.[6] Moreover, PLP deficiency has been associated with neurological disorders such as epilepsy[7] and its abundance is a prognostic factor in cancer patients.[8] Microorganisms and plants are capable of PLP de novo biosynthesis while other higher organisms acquire vitamin B$_6$ from nutrition and convert the three vitamers to PLP.[9] In addition, all cells utilize a salvage pathway in which PL liberated from enzymatic turnover is

recycled.[10] The PLP salvage pathway consists of pyridoxal kinases (PLKs), which phosphorylate all three vitamers at the 5′-alcohol (Figure 1) and pyridoxine-5′-phosphate oxidase (PNPOx), which converts the 5′-phosphorylated PNP and PMP to PLP.

PLKs belong to the enzyme family of ribokinases, which are transferases that catalyze the phosphorylation of a primary alcohol group on small aromatic molecules or carbohydrates.[11] For productive vitamer phosphorylation, PLKs undergo a conformational change to a state where the ATP γ-phosphate and substrate interact.[10,12] Eukaryotic and prokaryotic PLKs utilize a conserved basic residue (Cys or Asp)[12–14] in the active site that deprotonates the vitamer 5′-hydroxy group and enhances its nucleophilicity for an inline displacement of the
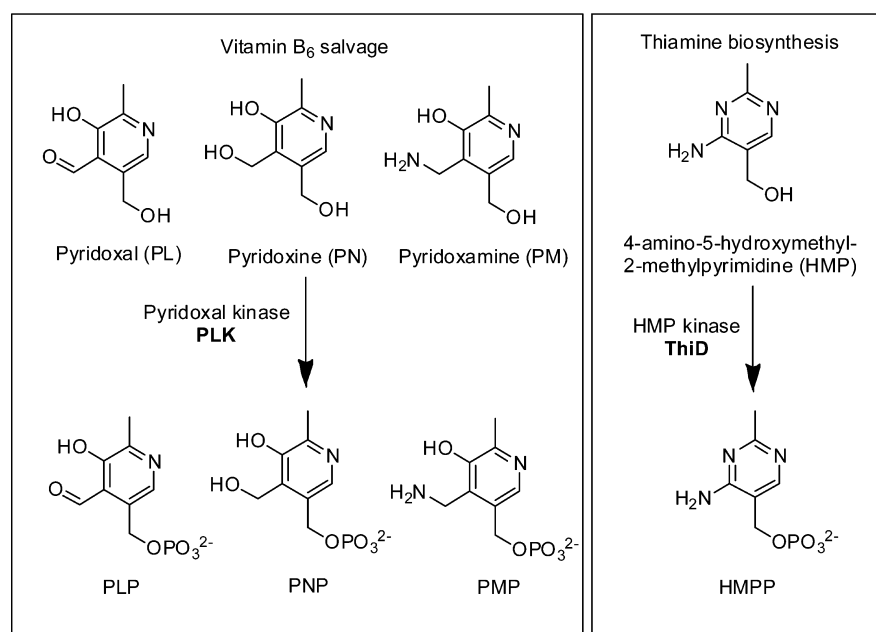
Figure 1. Left panel: Structues of the B_6 vitamers, PL, PN, and PM involved in vitamin B_6 salvage. Right panel: Structure of HMP involved in thiamine biosynthesis.

Table 1. Kinetic Parameters for SaThiD (SaPLK) WT, C110A, and C214D Turnover of PL, PN, and HMP[a]

	WT		C110A		C214D	
	K_m (μM)	k_{cat} (min^{-1})	K_m (μM)	k_{cat} (min^{-1})	K_m (μM)	k_{cat} (min^{-1})
PL	111 ± 53	9.88 ± 1.80	N/A	N/A	258 ± 68	19.7 ± 1.80
PN	2072 ± 332	0.95 ± 0.092	1508 ± 153	0.88 ± 0.047	N/A	N/A
HMP	1988 ± 268	2.73 ± 0.226	1848 ± 149	2.66 ± 0.112	N/A	N/A

[a]Phosphorylation of PN is also possible albeit with k_{cat} values lower than those of HMP and PL conversion (Table 1). N = 3, and ± represents standard deviation. N/A = no activty. For K_{cat}/K_m values, please refer to Supporting Information Table S1.

ATP γ-phosphate. During phosphoryl transfer, the substrates involved must be shielded from bulk solvent to prevent premature hydrolysis which is mediated through various mechanisms such as the formation of a dimeric β-clasp that acts as an active site lid,[15] through monomeric aggregation forming an active site between discrete units[16] or via flexible loops that cover the active site upon substrate binding.[12,17]

In a previous study, we identified an *Staphylococcus aureus* ribokinase (SaThiD) as a target of the cysteine-reactive natural product antibiotic rugulactone (Ru). Although this enzyme possesses an active site cysteine at position 214, the reactive Michael acceptor moiety of Ru selectively modified a remote cysteine at position 110 and led to covalent inhibition of phosphorylation.[18]

Here we report biochemical studies revealing that this *S. aureus* enzyme possesses significant activity toward both PL and the thiamine precursor HMP (Figure 1), giving this ribokinase a dual function in both the PL salvage and thiamine biosynthesis pathways. Functional studies further emphasize the importance of this kinase in the *S. aureus* PL salvage pathway. Additionally, we present high-resolution X-ray crystal structures of the *S. aureus* enzyme both with and without its substrates, and present a mechanism that explains the crucial role of a Cys 110/PL hemithioacetal for PL phosphorylation.

■ RESULTS

***S. aureus* ThiD (gi: 14246348, sav0580) Has Dual Function as an HMP and PL Kinase.** The evolution of ribokinases has yielded enzyme subfamilies that expand the scope of metabolite phosphorylation. For instance, HMP is phosphorylated twice by ThiD yielding HMP pyrophosphate, an essential precursor for thiamine biosynthesis (Figure 1).[19] However, due to the similarity of the pyridine and pyrimidine core structures, substrate promiscuity occurs. For example, Park and co-workers demonstrated that a predicted *Bacillus subtilis* ThiD showed higher activity for PL, and did not cluster with thiamine biosynthesis genes.[20] Prompted by this report, we determined the kinetic parameters for PL, PN, and HMP phosphorylation by SaThiD. We found that this enzyme had a K_m of only ~110 μM for PL compared to a K_m of ~2 mM for HMP (Table 1), while the turnover of both metabolites only differs by a factor of 3.6 (k_{cat} = 9.88 min^{-1} and k_{cat} = 2.73 min^{-1} for PL and HMP, respectively).

E. coli possesses two PL salvage enzymes, PdxK and PdxY, which share about 50% sequence identity.[13,14,21] A BLAST search of both the PdxK and PdxY sequences against *S. aureus* Mu50 or USA300 reveals only two comparable enzymes with about 20% sequence identity, both named ThiD. However, one ThiD (gi: 14247866) clusters with the thiamine biosynthesis operon, shares 29% sequence identity to *E. coli* ThiD (gi: 388478153), and is specifc for HMP.[22] In contrast, the other encoded by sav0580 (gi: 14246348), which we previously
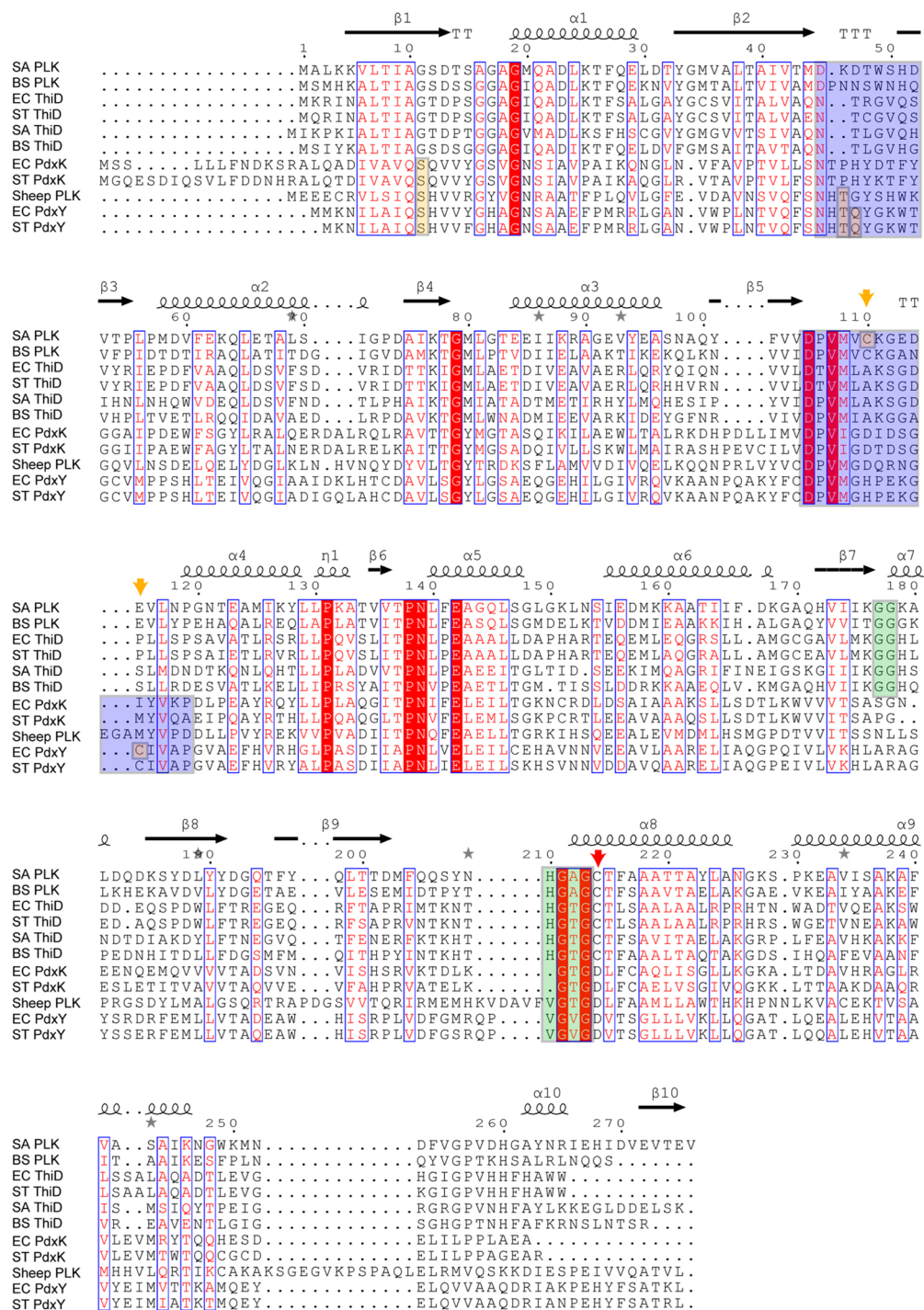
Figure 2. Structure based sequence alignment of *S. aureus* PLK (gi: 14246348), *E. coli* PdxK (gi: 388478462), *E. coli* PdxY (PDB code 1TD2), *S. thyphimurium* ThiD (gi: 1842118; PDB code 1JXH), *B. subtilis* PLK (gi: 16078236, PDB code 2I5B), sheep PLK (gi: 7387989, PDB code 1RFU). Sequences of *S. aureus* ThiD (gi: 14247866), *E. coli* ThiD (gi: 388478153), *S. thyphimurium* PdxK (gi: 20141744), *S. thyphimurium* PdxY (gi: 8159498), and *B. subtilis* ThiD (gi: 16080853) where there are no structural data available were aligned based on sequence homology. Highlighted in orange are residues directly interacting with the substrate; in green are the GG-switch region and anion hole. The active site closing flap is colored in blue. The catalytic acid is indicated by the red arrow. Annotation of secondary structure elements correspond to *S. aureus* PLK.

identified as target of rugulactone,[18] does not cluster with any of the thiamine biosynthesis genes *tenA*, *thiM*, and *thiE* in the *S. aureus* Mu50 and USA300 genomes (taxon: 158878 and 367830), and displays turnover of PL, HMP, and PN (Table 1), in line with the analogous *B. subtilis* enzyme reported by Park et al.[20]

To clarify the role of the enzyme encoded by sav0580 in live cells, we first examined the extracellular PL concentration of *S. aureus* USA300 WT and the transposon mutants TnThiD (sav0508 transposon) and TnPdxS (deficient in PLP de novo biosynthesis) after a 24 h growth period in a synthetic medium. The TnThiD mutant displayed an increase in extracellular PL levels compared to those of the WT and TnPdxS strains
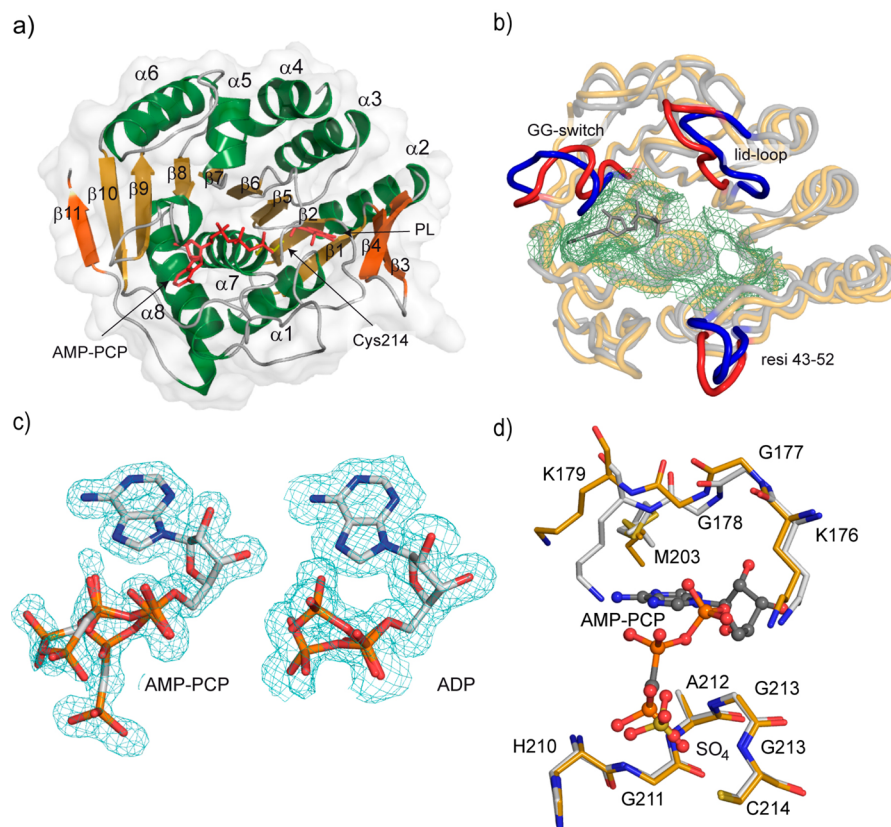
Figure 3. Folding topology and substrate binding of SaPLK. (a) Schematic representation of the SaPLK tertiary structure with the large central β-sheet and the flanking α-helices common to all ribokinases are shown in golden and green, respectively. The additional beta strands unique to SaPLK are highlighted in orange. A semitransparent surface representation of the protein is overlaid onto the model. AMP-PCP and PL are drawn as red sticks. (b) Superposition of *S. aureus* (golden/red) and *B. subtilis* PLK (PDB code 2I5B; gray/blue), highlighting the structural similarities and differences (red/blue). The binding pocket is indicated in green. (c) Simulated annealing-omit Fo-DFc electron density of the ATP analogue AMP-PCP and ADP in the SaPLK-complex structures, showing the multiple conformations of the β- and γ-phosphates. (d) In the superposition of unliganded-PLK (golden) and in complex with AMP-PCP (gray), the conformational change of the GG-switch region (residues 177−178) upon substrate binding is apparent. The γ-phosphate of AMP-PCP interacts with the preformed anion hole (residue 210−213). In the unliganded structure, this place is taken up by a sulfate from the crystallization conditions.

(Supporting Information Figure S1). This extracellular accumulation of PL in the strain lacking ThiD (sav0580), but competent in PLP de novo biosynthesis, demonstrates that sav0580 is performing PL to PLP salvage from the extracellular medium. Next, we compared growth of *S. aureus* USA300 WT, TnThiD (sav0580), and TnPdxS in synthetic medium in the presence and absence of PL. The data shows that TnPdxS displays little to no growth in the absence of PL, while in the presence of extracellular PL the TnPdxS mutant grows to the same extent as the WT, indicating that in the absence of de novo PLP synthesis vitamer salvage can compensate, resulting in WT-like growth (Supporting Information Figure S2). Finally, we compared the minimum inhibitory concentration (MIC) of the inhibitor Ru against *S. aureus* USA300 WT with that of the transposon mutants TnThiD (sav0580) and TnPdxS. While the MIC of Ru against USA 300 WT and TnThiD (sav0580) remained equal (~275 μM), the MIC of Ru for TnPdxS was decreased (~175 μM), indicating an impairment of PL salvage via inhibition of ThiD (sav0580) by Ru which cannot be compensated for by the inactivated de novo biosynthesis pathway (Supporting Information Figure S3).

This data suggests that the current *S. aureus* enzyme ThiD (gi: 14246348, sav0580) designation as a thiamine biosynthesis enzyme can be expanded to include PL salvage. As this dual-function enzyme displays a higher turnover for PL than for

HMP, and is not found in the thiamine biosynthesis operon, we will refer to this enzyme as SaPLK. A sequence alignment of the *E. coli* (ThiD, PdxK, PdxY) as well as the respective *S. aureus* and *B. subtilis* enzymes (ThiD, PLK) is shown Figure 2.

Cys 110 in SaPLK Has Elevated Reactivity. In our previous report, we demonstrated that the Michael-acceptor containing natural product Ru modified Cys 110 of SaPLK in a whole-cell labeling experiment, indicating that Cys 110 of SaPLK is of elevated reactivity. This covalent attachment further resulted in the inhibition of enzymatic activity.[18] In order to validate the importance of this residue for Ru binding and the corresponding inhibition of enzyme activity, we compared turnover of PN by SaPLK WT and SaPLK C110A in the presence of Ru. As expected, while Ru inhibited the turnover of PN by SaPLK WT to the same extent as previously reported (apparent IC$_{50}$ ∼ 15 μM), it did not inhibit the turnover of PN by the C110A variant at any concentration tested (max [Ru] = 180 μM) (Supporting Information Figure S4).

Cys 214 Is the Catalytic Base of SaPLK, while Cys 110 Is Mandatory for PL, but Not PN or HMP Turnover. Comparison of SaPLK with structures of known ribokinases shows that Cys 214 is in the active site acting as the catalytic residue, and Cys 110 is positioned in an active site shielding, flexible "lid" loop (Figure 2).
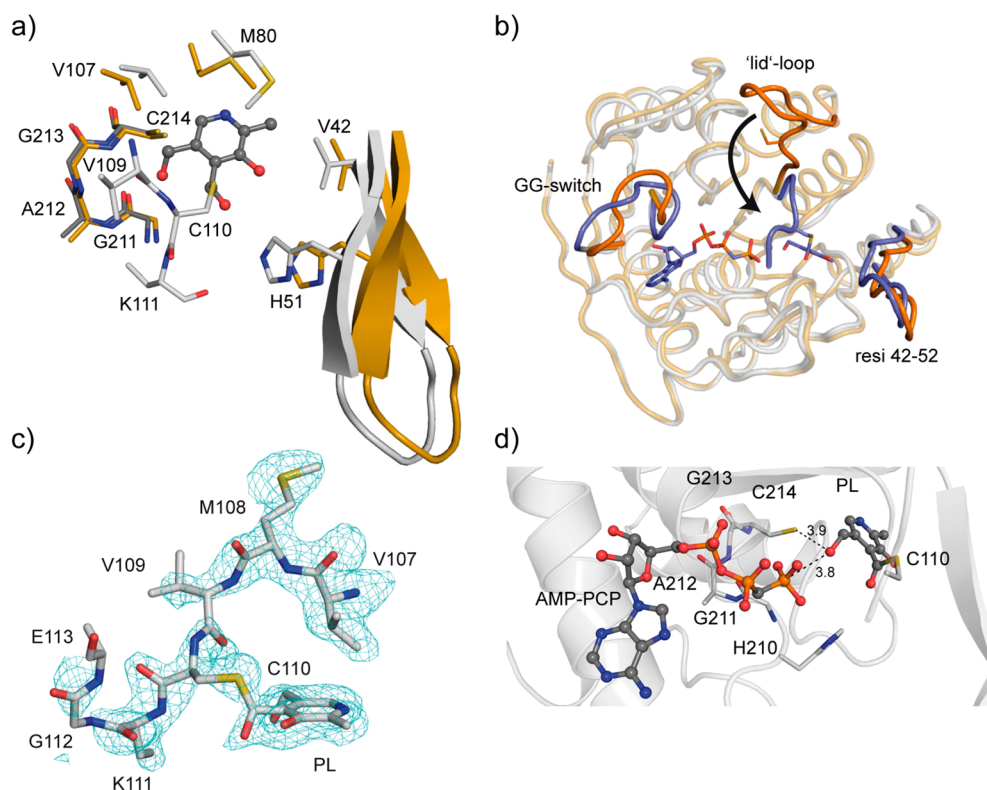
Figure 4. Binding of pyridoxal by SaPLK. (a) Conformational changes upon PL binding (unliganded-PLK golden, SaPLK/PL gray, PL shown as ball and stick model). (b) Superpostion of unliganded (golden/red) and AMP-PCP/PL bound SaPLK (gray/blue) highlighting the conformational changes. (c) Simulated annealing-omit Fo-DFc electron density of PL and hemithioacetal formation with the active-site closing loop in the PL-complex. (d) AMP-PCP and PL bound to SaPLK. Residues of the anion hole and Cys 110 are shown as stick model.

In order to decipher the mechanistic roles of these two residues in greater detail, several SaPLK variant proteins were prepared, and their kinetic parameters determined (Table 1). We found that the C214A variant did not turn over PL, PN, or HMP under any conditions, providing further evidence that this residue acts as the catalytic base in the phosphorylation reaction. Cys 214 can be functionally replaced by a basic aspartate as in the PLKs from Gram-negative bacteria or eukaryotes (Figure 2).[12−14] The SaPLK C214D variant retained full activity against PL, but lost its ability to phosphorlylate PN. Meanwhile, the C110A variant protein displayed approximately equal kinetics toward PN and HMP yet was surprisingly inert toward PL (Table 1). Taken together this suggests a key role of Cys 110 in PL phosphorylation.

SaPLK Exhibits a Ribokinase Fold. In order to elucidate the SaPLK reaction mechanism and the role of Cys 110, we determined the X-ray crystal structures of SaPLK alone and in complex with its substrates to 1.4−1.85 Å resolution. Unliganded SaPLK shows a typical ribokinase fold[11] with a central large β-sheet consisting of nine strands, flanked by three and five structurally conserved α-helices (Figure 3a).

The active biomolecule consists of a homodimer, and two homodimers can be found in the asymmetric unit of the crystal (Supporting Information Figure S5a); 1850 Å^2 ($\sim$15% of the surface) is buried in the dimer interface. Deviation of the four protein chains in each crystal structure is small, and they can be superimposed with an rmsd of 0.2 Å (Supporting Information Figure S5b,c). The loops between sheet 3 and 4 (residues 43−52) and between sheet 6 and helix 4 (residues 109−116) are extended and form a flap, shielding the active site from the solvent (Figure 3b). Cys 110 resides in this flexible active-site

closing loop. In all but one molecule where it is engaged in crystal lattice contacts, this loop is flexible and no electron density can be observed (Figure 3b). Similar observations have been made in the structures of *B. subtilis* PLK[23] and *S. thyphimurium* ThiD.[17]

Characteristic PL and ATP Binding Motifs in SaPLK. To investigate substrate recognition, SaPLK was cocrystallized with ADP and AMP-PCP (a nonhydrolyzable analogue of ATP). In addition, PL was added to the mother liquor of unliganded-SaPLK and SaPLK/AMP-PCP cocrystals. Electron difference density for the substrates could be clearly observed in the active sites of all protein chains in the asymmetric unit of the crystal after the initial round of refinement (Figure 3c).

Binding of ATP and/or PL to SaPLK resulted in two distinct conformational states that added up to an overall active enzyme−substrate complex. The rmsd between unliganded and substrate-bound SaPLK is about 0.5 Å. In the SaPLK/ADP and SaPLK/AMP-PCP cocrystal structures, Gly-Gly residues 177−178 ("GG-switch" region)[24] undergo a torsion angle change to engage with the adenine moiety (Figure 3d). This is also accompanied by an ordering of residues 204−208 at the Watson−Crick face of the purine moiety. Met 203 alternates its rotamer and packs over the aromatic ring (Figure 3d). Such sulfur−arene interactions are commonly observed in protein−ligand complexes where they contribute stabilizing hydrophobic, steric, and dispersion effects to substrate binding.[25]

Located on the opposite end of the ATP binding groove is the PL substrate pocket (Supporting Information Figure S6b). In all structures obtained, PL is bound to the same position independent from AMP-PCP binding or the conformational state of the active site closing loop (Supporting Information
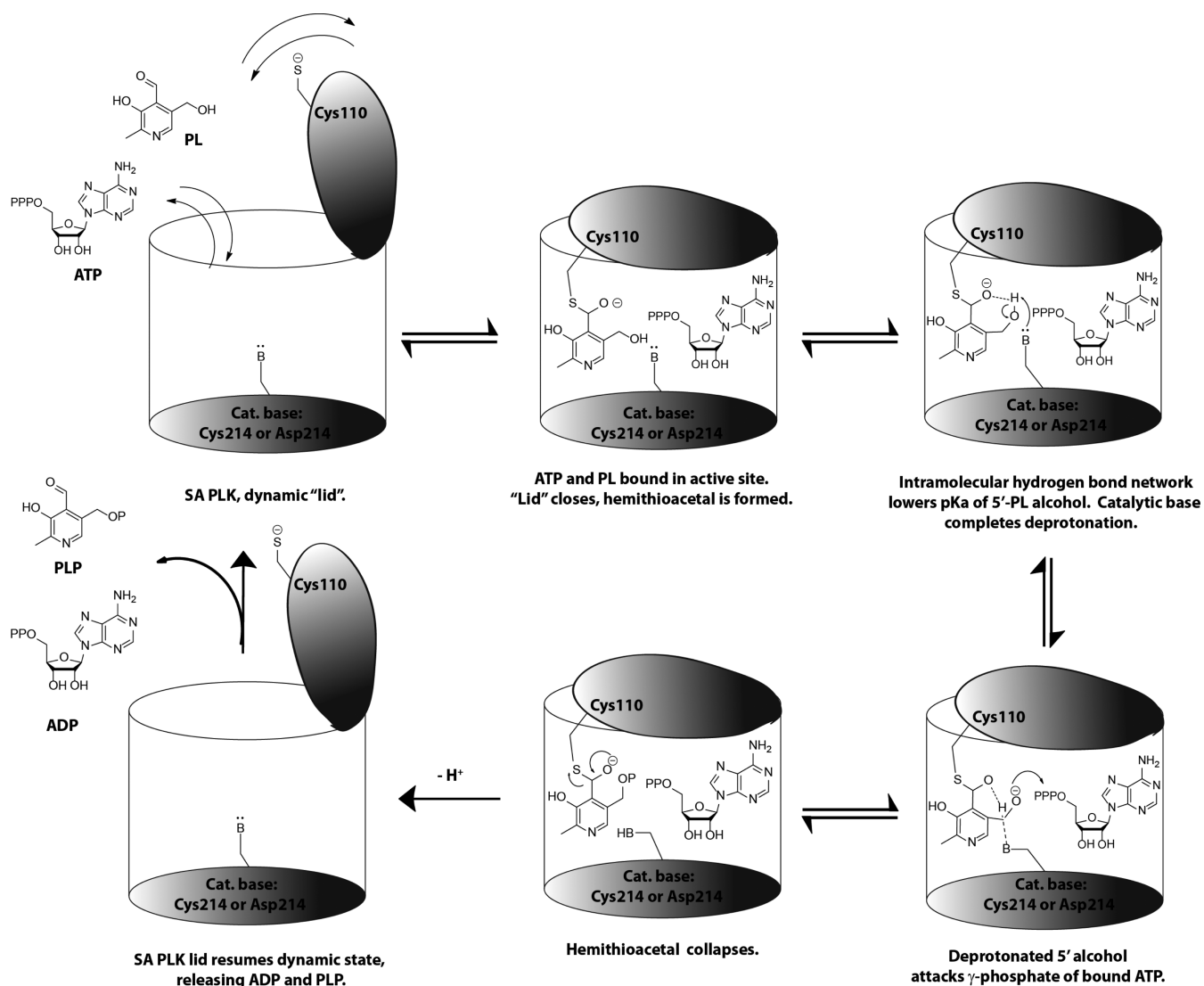
Figure 5. Proposed mechanism for PL turnover by CC-PLKs.

Figure S6b). This position is structurally equivalent to the substrate-binding site in other PLK and ThiD enzymes. Moreover, the substrate binding sites are highly conserved in SaPLK homologues (Supporting Information Figure S6a). To improve the substrate fit, Met 80 rotates on top of the pyridine ring (Figure 4a).

PL Forms a Hemithioacetal with SaPLK Cys 110. PL binding causes the β-hairpin formed by residues 42–52 to move closer to the PL edge, shielding it further from nucleophilic attack by the bulk solvent (Figure 4a). Importantly, upon PL binding the active site closing "lid" loop swings in and formation of a hemithioacetal of Cys 110 with the aldehyde group of PL (Figure 4b,c and Supporting Information Figure S7) is observed in two of the four molecules in the asymmetric unit of the crystal.

Due to crystal lattice effects, this loop closure and partial ordering of the loop did not occur in all protein molecules of the asymmetric unit. Apart from the hemithioacetal formation, PL is held in its binding pocket by hydrophobic packing interactions as well as water-mediated contacts (Supporting Information Figure S7a).

Once the substrate is locked in place, the 5′-hydroxy group can carry out a nucleophilic attack on the γ-phosphate of ATP

leading to a negatively charged intermediate (Figure 4d). The charge is balanced by an anion hole as observed in the unliganded and ADP complex structures (taken up by a sulfate ion from the crystal mother liquor) at the coil-to-helix transition (residues 211–214) (Figure 3d). However, the strained conformation and positioning of the γ-phosphate of the AMP-PCP at the anion hole is not favorable, since the methylene bridge of this ATP-analogue is forced to interact with the peptide backbone nitrogens of the anion hole residues Ala 212 and Gly 213. Thus, the γ-phosphate is not fully elongated and its distances to the PL 5′-hydroxy group and Cys 214 are about 4 Å (Figure 4d). In the case of the real substrate ATP, the favored interaction between the bridging oxygen and the anion hole most likely results in stretching-out of the ATP phosphate tail, thus shortening the distance to the substrate and enabling efficient phosphate transfer. The complex structure of SaPLK with AMP-PCP and PL combines the conformational changes observed upon separate binding of the substrates (Figure 4b).

It has been previously shown that mono- or divalent metal ions, such as K^+, Zn^{2+},[12] and Mg^{2+},[24] are essential for catalysis in many kinases, where their concerted action is the driving force for ATP binding and substrate catalysis.[26–28] Accordingly,

4997

dx.doi.org/10.1021/ja411785r | J. Am. Chem. Soc. 2014, 136, 4992–4999

the crystal structure shows electron density in the vicinity of the AMP-PCP/ADP phosphate groups, which was modeled as a water molecule since no Mg^{2+} was present in the crystallization conditions (Supporting Information Figure S8).

"CC-PLKs": A Subclass of Pyridoxal Kinases? A BLAST search[29] revealed that both Cys residues are conserved in a large number of homologous enzymes that are unique to the phyla of Fusobacteria, Actinobacteria, and Firmicutes (Supporting Information Figure S9). We thus cloned and purified homologous proteins from *Listeria monocytogenes* (LmPLK) and *Enterococcus faecalis* (EfPLK), which share 59% and 52% sequence identity with SaPLK, respectively. These enzymes feature the Cys 110 and Cys 214 residues and phosphorylate PL. LmPLK displays similar behavior to SaPLK; the WT shows a considerable preference for PL over PN, and the C110A variant loses almost all activity toward PL while retaining PN turnover equal to that of the WT. Meanwhile, EfPLK WT displays approximately equal turnover of PL and PN, but the C110A variant of this protein has little activity toward PL while preserving PN turnover (Supporting Information Figure S10). This data implies that the "CC-PLK" class of pyridoxal kinases operates through a shared mechanism (see below).

■ DISCUSSION

Hemithioacetal Formation Drives PL Phosphorylation by a Unique Mechanism. Based on the data presented here, we propose the following reaction mechanism for the conversion of PL to PLP by SaPLK (Figure 5). First, binding of PL and ATP into the active site results in reshaping of the binding pocket (GG-switch conformational change, ordering of loop 204−208 and wedging-in of β-hairpin residues 42−52) and aligning of the phosphate tail of ATP with the substrate, the catalytic base, and the anion hole. Second, the flexible lid loop closes and a hemithioacetal with PL is formed. This lid closure shields the active site from the bulk solvent. Third, the formation of the hemithioacetal in the active site results in a developing negative charge on the 4′-oxygen atom of PL (Figure 5).

The developing negative charge can then act to lower the pK_a of the PL 5′-alcohol. This increase in alcohol acidity via an intramolecular hydrogen bonding network between two oxygen atoms has been observed for several aliphatic and aromatic systems, often with dramatic decreases in pK_a.[30−34] Such an activation also occurs in the enolization of 2′-carboxyphe-nones.[35−37] The intramolecular activation of the 5′-alcohol is then completed by the catalytic base at position 214, followed by the nucleophilic displacement of the γ-phosphate of the bound ATP. Because the 5′-alcohol has been partially acidified by an intramolecular mechanism, both a strong (Cys, $pK_a \sim 9$) and weak (Asp, $pK_a \sim 4$) base can complete the deprotonation of the alcohol and the subsequent formation of PLP. Finally, the hemithioacetal collapses, and the "lid" opens, releasing PLP and ADP. Thus, the charge present on the nucleophilic Cys 110 is transferred to the 4′-alcohol of the bound PL molecule, increasing its hydrogen bond acceptor strength.

In the case of PN turnover, a hemithioacetal cannot be formed. Because there is no negative charge to lower the pK_a of the 5′-alcohol of the substrate, a weaker base (as in the C214D variant) cannot complete the deprotonation of the 5′-alcohol and phosphorylation of PN does not occur in this variant. As mentioned above, other PLKs are capable of utilizing an Asp residue to phosphorylate PL without the benefit of hemi-thioacetal formation. In SaPLK, apart from the hemithioacetal,

there are no direct interactions between the PL substrate and the enzyme (Supporting Information Figure S7). In contrast, in the *E. coli* PdxK, Ser 28 forms a H-bond to the pyridine nitrogen and Nε2 of His 59 is close (3.3 Å) to the PL 5′-hydroxy group (Supporting Information Figure S11). The interaction of His 59 with the 5′-hydroxy group of PL can serve to acidify this proton, thus facilitating phosphorylation by the catalytic Asp in this enzymatic species.

Dual Function CC-Pyridoxal Kinases Combine Features from *E. coli* ThiD, PdxK, and PdxY. We have thus far described a ribokinase in *S. aureus* that acts as a dual function PL and HMP kinase, and which phosphorylates PL by a distinctive intramolecular activation of the PL 5′-hydroxy group. When compared to the three *E. coli* ribokinases responsible for PL salvage (PdxK, PdxY) and HMP phosphorylation (ThiD), it would appear that SaPLK combines structural and functional features from these three enzymes. In *E. coli* PdxY, a hemithioacetal formation between a Cys residue in the active site closing loop with the aldehyde group of PL was previously observed.[14] The position of the lid-loop Cys in PdxY is located five residues upstream compared to SaPLK, LmPLK, and EfPLK (Figure 2 and Supporting Information Figure S9). In contrast to the Cys 214 base in SaPLK, an aspartate (Asp 224) in PdxY acts as the catalytic base for substrate deprotonation. Finally, the interactions between kinase and substrate differ substantially between SaPLK and *E. coli* PdxY. (Supporting Information Figures S7 and S11).

Like PdxY, *E. coli* PdxK uses an aspartate as the catalytic base. However, in PdxK, no cysteine residue is present in the lid loop as in SaPLK. Furthermore, the architecture of the lid loop in PdxK is different from that of SaPLK, resulting in a distinct active site closure mechanism (Supporting Information Figure 11).

While full structural details from *E. coli* ThiD are not yet available, this enzyme, like SaPLK, uses a cysteine residue as its catalytic base.

Structurally, SaPLK combines features from *E. coli* PdxY (lid loop cysteine forms a hemithioacetal with PL) and *E. coli* ThiD (cysteine as catalytic base). PdxK has been reported to be the main PL salvage enzyme in *E. coli*, with PdxY playing a minor role in vitamer salvage.[21,38] Therefore, SaPLK combines functionality from both *E. coli* PdxK and ThiD in that it turns over both PL and HMP. This combination of features manifests itself as the CC-PLKs fulfilling a dual function as both an HMP and a PL kinase.

■ CONCLUSION

In conclusion, we report a novel class of pyridoxal kinases which utilize a hemithioacetal for pyridoxal to pyridoxal-5′-phosphate turnover. High-resolution crystal structures of a representative of this enzymatic class from *S. aureus* (SaPLK) in its unliganded as well as substrate-bound forms clearly show the interaction of a non-active-site cysteine with pyridoxal in the form of a hemithioacetal. These structures, combined with biochemical data, allow us to propose a mechanism of pyridoxal phosphorylation in this class of ribokinases. Furthermore, we validate the inhibition of SaPLK by the natural product antibiotic rugulactone, and the impact of this inhibition on the bacterial PLP salvage pathway. The elucidation of the structure and mechanism of SaPLK offers opportunities for rational inhibitor design upon a novel target. In addition to designing analogues to impair the bacterial vitamin B_6 salvage pathway, alternate strategies can also be explored. For example, a recent

report describes the application of synthetic PL analogues to *Plasmodium falciparum*, which after uptake are phosphorylated by PfPLK and thus trapped in the parasitic cytosol. These phosphorylated PL analogues can then act to poison a multitude of PLP-dependent enzymes in the cell.[39] The structure and mechanism of the vitamin B_6 salvage enzyme from multidrug resistant *Staphylococcus aureus* disclosed in this report will assist in targeting novel ways to combat this dangerous pathogen.

■ ASSOCIATED CONTENT

Ⓢ Supporting Information

Detailed experimental procedures, PDB codes, data processing and structure refinement statistics, and supplementary figures and schemes. This material is available free of charge via the Internet at http://pubs.acs.org.

■ AUTHOR INFORMATION

Corresponding Authors
sabine.schneider@tum.de
stephan.sieber@tum.de
Notes
The authors declare no competing financial interest.

■ ACKNOWLEDGMENTS

■ REFERENCES

(1) Eliot, A. C.; Kirsch, J. F. *Annu. Rev. Biochem.* **2004**, *73*, 383−415.
(2) Percudani, R.; Peracchi, A. *EMBO Rep.* **2003**, *4*, 850−854.
(3) El Qaidi, S.; Yang, J.; Zhang, J. R.; Metzger, D. W.; Bai, G. *J. Bacteriol.* **2013**, *195*, 2187−2196.
(4) Grubman, A.; Phillips, A.; Thibonnier, M.; Kaparakis-Liaskos, M.; Johnson, C.; Thiberge, J. M.; Radcliff, F. J.; Ecobichon, C.; Labigne, A.; de Reuse, H.; Mendz, G. L.; Ferrero, R. L. *mBio* **2010**, *1*, e00112−10.
(5) Dick, T.; Manjunatha, U.; Kappes, B.; Gengenbacher, M. *Mol. Microbiol.* **2010**, *78*, 980−988.
(6) Kelly, R. C.; Bolitho, M. E.; Higgins, D. A.; Lu, W.; Ng, W. L.; Jeffrey, P. D.; Rabinowitz, J. D.; Semmelhack, M. F.; Hughson, F. M.; Bassler, B. L. *Nat. Chem. Biol.* **2009**, *5*, 891−895.
(7) Bahi-Buisson, N.; Dulac, O. *Handb. Clin. Neurol.* **2013**, *111*, 533−541.
(8) Galluzzi, L.; Vacchelli, E.; Michels, J.; Garcia, P.; Kepp, O.; Senovilla, L.; Vitale, I.; Kroemer, G. *Oncogene* **2013**, *32*, 4995−5004.
(9) Mooney, S.; Leuendorf, J. E.; Hendrickson, C.; Hellmann, H. *Molecules* **2009**, *14*, 329−351.
(10) di Salvo, M. L.; Contestabile, R.; Safo, M. K. *Biochim. Biophys. Acta* **2011**, *1814*, 1597−1608.
(11) Park, J.; Gupta, R. S. *Cell. Mol. Life Sci.* **2008**, *65*, 2875−2896.
(12) Li, M. H.; Kwok, F.; Chang, W. R.; Liu, S. Q.; Lo, S. C.; Zhang, J. P.; Jiang, T.; Liang, D. C. *J. Biol. Chem.* **2004**, *279*, 17459−17465.
(13) Safo, M. K.; Musayev, F. N.; di Salvo, M. L.; Hunt, S.; Claude, J. B.; Schirch, V. *J. Bacteriol.* **2006**, *188*, 4542−4552.
(14) Safo, M. K.; Musayev, F. N.; Hunt, S.; di Salvo, M. L.; Scarsdale, N.; Schirch, V. *J. Bacteriol.* **2004**, *186*, 8074−8082.
(15) Sigrell, J. A.; Cameron, A. D.; Jones, T. A.; Mowbray, S. L. *Structure* **1998**, *6*, 183−193.
(16) Campobasso, N.; Mathews, I. I.; Begley, T. P.; Ealick, S. E. *Biochemistry* **2000**, *39*, 7868−7877.
(17) Cheng, G.; Bennett, E. M.; Begley, T. P.; Ealick, S. E. *Structure* **2002**, *10*, 225−235.
(18) Nodwell, M. B.; Menz, H.; Kirsch, S. F.; Sieber, S. A. *ChemBioChem* **2012**, *13*, 1439−1446.
(19) Begley, T. P.; Downs, D. M.; Ealick, S. E.; McLafferty, F. W.; Van Loon, A. P.; Taylor, S.; Campobasso, N.; Chiu, H. J.; Kinsland, C.; Reddick, J. J.; Xi, J. *Arch. Microbiol.* **1999**, *171*, 293−300.
(20) Park, J. H.; Burns, K.; Kinsland, C.; Begley, T. P. *J. Bacteriol.* **2004**, *186*, 1571−1573.
(21) di Salvo, M. L.; Hunt, S.; Schirch, V. *Protein Expression Purif.* **2004**, *36*, 300−306.
(22) Müller, I. B.; Bergmann, B.; Groves, M. R.; Couto, I.; Amaral, L.; Begley, T. P.; Walter, R. D.; Wrenger, C. *PLoS One* **2009**, *4*, e7656.
(23) Newman, J. A.; Das, S. K.; Sedelnikova, S. E.; Rice, D. W. *J. Mol. Biol.* **2006**, *363*, 520−530.
(24) Schumacher, M. A.; Scott, D. M.; Mathews, I. I.; Ealick, S. E.; Roos, D. S.; Ullman, B.; Brennan, R. G. *J. Mol. Biol.* **2000**, *298*, 875−893.
(25) Meyer, E. A.; Castellano, R. K.; Diederich, F. *Angew. Chem., Int. Ed. Engl.* **2003**, *42*, 1210−1250.
(26) Baez, M.; Cabrera, R.; Pereira, H. M.; Blanco, A.; Villalobos, P.; Ramirez-Sarmiento, C. A.; Caniuguir, A.; Guixe, V.; Garratt, R. C.; Babul, J. *Biophys. J.* **2013**, *105*, 185−193.
(27) Di Cera, E. *J. Biol. Chem.* **2006**, *281*, 1305−1308.
(28) Musayev, F. N.; di Salvo, M. L.; Ko, T. P.; Gandhi, A. K.; Goswami, A.; Schirch, V.; Safo, M. K. *Protein Sci.* **2007**, *16*, 2184−2194.
(29) Altschul, S. F.; Gish, W.; Miller, W.; Myers, E. W.; Lipman, D. J. *J. Mol. Biol.* **1990**, *215*, 403−410.
(30) Tian, Z.; Fattahi, A.; Lis, L.; Kass, S. R. *J. Am. Chem. Soc.* **2009**, *131*, 16984−16988.
(31) Shan, S. O.; Herschlag, D. *Proc. Natl. Acad. Sci. U.S.A.* **1996**, *93*, 14474−14479.
(32) Shan, S. O.; Loh, S.; Herschlag, D. *Science* **1996**, *272*, 97−101.
(33) Shokri, A.; Abedin, A.; Fattahi, A.; Kass, S. R. *J. Am. Chem. Soc.* **2012**, *134*, 10646−10650.
(34) Shokri, A.; Schmidt, J.; Wang, X. B.; Kass, S. R. *J. Am. Chem. Soc.* **2012**, *134*, 2094−2099.
(35) Bell, R. P.; Covington, A. D. *J. Chem. Soc.* **1975**, *2*, 1343−1348.
(36) Harper, E. T.; Bender, M. L. *J. Am. Chem. Soc.* **1965**, *87*, 5625−5632.
(37) Bell, R. P.; Cox, B. G.; Henshall, J. B. *J. Chem. Soc., Perkin Trans. 2* **1972**, 1232−1237.
(38) Yang, Y.; Tsui, H. C.; Man, T. K.; Winkler, M. E. *J. Bacteriol.* **1998**, *180*, 1814−1821.
(39) Müller, I. B.; Wu, F.; Bergmann, B.; Knockel, J.; Walter, R. D.; Gehring, H.; Wrenger, C. *PLoS One* **2009**, *4*, e4406.